A series-parallel hybrid electric powertrain for industrial vehicles

Sergio Grammatico
Department of Electrical
Systems and Automation, University of Pisa
Largo Lucio Lazzarino 1, 56127 Pisa, Italy
email: s.grammatico@dsea.unipi.it

Andrea Balluchi
Pure Power Control s.r.l
Via Giuntini 63
56023 Navacchio (PI), Italy
email: andrea@purepowercontrol.com

Ettore Cosoli
Dana Italia s.p.a
Zona Industriale Lifano 15
38062 Arco (TN), Italy
email: ettore.cosoli@dana.com

***Abstract*—In the last years there is a growing interest in electric and hybrid electric propulsions due to environmental concerns. In particular industrial vehicles are a promising field of application for their duty cycles characterized by low velocities, frequent start and stop jobs, long periods of idling and material-handling tool power peaks. In this paper a series-parallel hybrid electric powertrain for wheel loaders is investigated with the goal to reduce the fuel consumption. The developed architecture exploits the benefits of a series hybrid electric powertrain at low traction requirements and progressively takes advantage from the typical power coupling of a parallel hybrid drivetrain at increasing power demands, according to the ordinary employment of a loader. In the drivetrain, a planetary gear unit and the electrical subsystem (generator/motor and battery) decouple the wheels from the engine operating point. Therefore the supervisory regulator can control the engine in its high efficiency regions. The drivetrain is modeled and a control algorithm is derived. Simulation results confirm the attractiveness of the proposed series-parallel hybrid electric powertrain for loaders.**

I. Introduction

Nowadays Hybrid Electric Vehicles (HEVs) are recognized as one the most promising technologies in significantly reducing the petroleum fuel consumption, toxic and greenhouse gases emissions [1]. Hybrid powertrains use at least two energy sources for their propelling; usually, an Internal Combustion Engine (ICE) is assisted by one Electric Generator (EG) and one Electric Motor (EM), which use an electrochemical battery as energy storage. The fundamental hybrid electric drivetrain architectures are the series configuration, in which the energy sources are coupled together electrically through a DC bus and the parallel configuration, in which energy sources are coupled together mechanically [2]. The series hybrid powertrain has its foremost advantage in the fact that the engine is mechanically decoupled from the vehicle wheels so it can be operated in its high efficient speed and torque region. Its main disadvantage is that mechanical power from the engine changes its form twice, from mechanical to electrical in the electric generator and from electrical to mechanical again in the electric motor. From this point of view, in a parallel hybrid electric powertrain the engine can deliver torque directly to the wheels without undergoing energy form change. The major disadvantage of a parallel configuration is that the engine cannot be always controlled in its high efficiency operating region because it is still mechanically coupled to the wheels.

Series hybrid electric powertrain control was deeply studied in the literature, for instance through dynamic programming [3] and minimization strategies [4], [5], [6]. Also for the parallel hybrid electric architecture, optimization techniques [7], [8], [9] have been fully exploited.

To overcome the disadvantages of series and parallel architectures, many series-parallel hybrid powertrains have been developed and tested. The main idea is to take advantage of both an electric and a mechanical coupling mechanisms in the drivetrain [1]. The Toyota Hybrid System (THS) [10], [11] became one of the most famous series-parallel architecture because it allows good performances at all power demands of a car driver. The power management problem [12] was tackled through static optimization techniques and, more generally, in an optimal control theory setting. In [13], [14] the Equivalent Consumption Minimization Strategy (ECMS) was presented as an optimal strategy in energy management on HEVs. As can be seen from the THS model [11], drivetrains equipped with a planetary gear unit have got mixed relationships between input torques and output speeds; furthermore the main disadvantage of a series-parallel hybrid architecture is that the presence of both a mechanical coupling and a planetary gear unit results in extra power loss.

As for industrial vehicles, purely electric propulsion systems are widely adopted for lightweight vehicles, such as fork-lift trucks. Some fork-lift trucks equipped with either Diesel-electric or series hybrid electric propulsion have been recently introduced to the market; instead the process of hybridization is much slower for heavy duty loaders. For them, many practical situations with high power requirements, for example due to the additional bucket tasks, should be profitable for a parallel hybrid architecture, while a series configuration probably remains the best choice in performing low-power jobs, for instance transfers at relatively low longitudinal speed.

In this paper a series-parallel architecture is designed for the propulsion of a wheeled front-end loader. The main aim is the reduction of the fuel consumption. The novelty of the proposed solution regards the fact that a non ordinary series-parallel hybrid electric propulsion system is here fitted to an off-road heavy duty loader, whose powertrains are usually

978-1-4244-8218-4/10/$26.00 ©2010 IEEE

Fig. 1. Compact wheel loader.

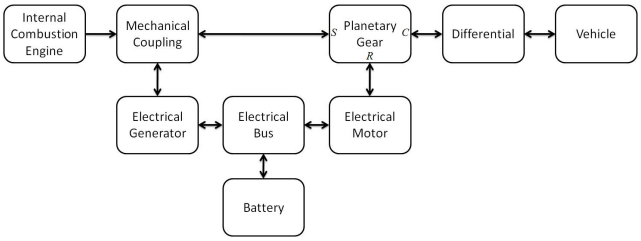

Fig. 2. Series-parallel hybrid electric powertrain scheme. The mechanical coupling between the ICE and the EG is connected to the sun shaft, the EM to the ring shaft and the carrier shaft is connected to the differential. The proposed architecture is input-coupled output-split, while the THS is an input-split output-coupled solution.

conventional ones or at most hydrostatic [15], [16]. Series and parallel hybrid electric powertrains for trucks have been recently investigated in [6] and [8].

The paper is organized as follows. In Section 2 the case of study is showed and the proposed series-parallel hybrid electric powertrain is presented, pointing out the differences with respect to the well-known THS. In Section 3 we describe the control strategy to maintain the ICE in its high efficiency operating region and to decouple the input-output dynamics in the Multiple Input Multiple Output (MIMO) drivetrain. Performed simulations show the behavior of the overall propulsion system for the typical duty cycles of loaders. In the last section we conclude the paper and summarise our work.

II. The Proposed Series-Parallel Hybrid Electric Powertrain

Several series-parallel hybrid electric architectures can be conceived with planetary gear units, e.g. input-coupled, output-coupled and compound. The success of THS was due to the fact that it is practically ideal for the broad range of possible operating conditions of a car. In particular the THS power-split is a good trade-off between urban cycles paths and suburban ones. At ordinary vehicle speeds, up to very high speeds on highway, the powertrain behavior become very similar to a high-efficiency parallel hybrid architecture, while at low speeds the electrical subsystem is more useful for traction. The THS is just one example of *input-split output-coupled* powertrains [17].

Conversely, industrial loaders, see Figure 1, always work at low speeds and need high torques, for instance in a full-load bucket handling and in quick full-load accelerations. Moreover, the major part of their life is spent in idling conditions. Therefore for industrial vehicles it is preferable a series-parallel drivetrain that usually looks like a series architecture to maintain the ICE at high efficiency operating regions also at very low power demands; then the engine should also be able to directly deliver mechanical power to the wheels, thanks to the planetary gear unit, at high power requirements.

To handle such typical specifications of loaders, an *input-coupled output-split* series-parallel hybrid electric architecture is represented in Figure 2. The arrows point out the directions of possible power flows. Powertrain elements are connected to the planetary gear as follows: the mechanical coupling [2] between the ICE and the EG is connected to the sun shaft, the EM to the ring shaft and, finally, the carrier shaft is the output shaft. It is worth to note that unlike the classical series-parallel hybrid electric configurations [1], [11], here the electric generator shaft is not a shaft of the planetary gear unit. The EG of our powertrain is very close to the ICE, through a reduction gear of the mechanical coupling unit. As a result, we will see in Section 3 that the electric generator can be used to easily and directly control the engine load, because the generator torque do not go through the planetary gear unit, consequently it directly influences the engine shaft dynamics. The appeal of the proposed architecture is that the series power flow, from engine to electrical subsystem and finally to wheels, is fully exploited thanks to the EG control. When the vehicle performs relatively high speeds (15-20 km/h) or requests high powers, the powertrain behavior gradually shifts to a parallel hybrid electric one.

Many different drivetrain layouts have been investigated for off-road vehicles, e.g. agricultural tractors, especially for power split transmissions, including the idea to mechanically couple the engine at the sun shaft (input coupled transmission) with *hydrostatic* drives. For instance, see [15], [16] and the references therein. However, input-coupled output-split series-parallel hybrid electric powertrains have not been already investigated for medium and high weight industrial vehicles, at least at the authors' knowledge.

In the following we present the MIMO drivetrain model, according to the dynamic modeling approach [18]. Considering the planetary gear, let ω_r, ω_c and ω_s be the angular velocities of, respectively, the ring, the carrier and the sun shaft. If T_r, T_c and T_s are, respectively, the ring, the carrier and the sun torques, then the three constraints (1), (2) (one speed constraint and two torque constraints) hold.

$$\omega_s = (1+\rho)\omega_c - \rho\omega_r \tag{1}$$

where $\rho = z_r/z_s$ is equal to the teeth number of the ring gear over the sun gear one.

$$\begin{cases} T_r = \rho\eta_0^{\beta} T_s \\ T_c = \left(1 + \rho\eta_0^{\beta}\right) T_s \end{cases} \tag{2}$$

Here η_0^{β} is the efficiency from the sun gear to the ring gear when the carrier is fixed to the frame ($\omega_c = 0$), while the exponent β is such that it always determines energy losses.

$$\beta = \begin{cases} +1 & if\ T_s\left(\omega_c - \omega_r\right) > 0 \\ 0 & if\ T_s\left(\omega_c - \omega_r\right) = 0 \\ -1 & if\ T_s\left(\omega_c - \omega_r\right) < 0 \end{cases} \tag{3}$$

In the same setting of [10], we can write down the dynamic equations of each shaft. ω_w is the wheel rotational speed. T_{aux} is the torque required by the bucket handling pump, T_{fr} is a friction torque and T_{rr} is the rolling resistance torque at the wheels. Since in typical wheel loader duty cycles, the vehicle speed does not exceed 20 km/h, then aerodynamical forces are neglected. Furthermore, non longitudinal dynamics are also neglected, because the vehicle does not exhibit significant lateral dynamical transients.

The inputs of the dynamic model are the torques of the internal combustion engine T_e, of the electric motor T_m and of the electric generator T_g. The outputs (and state variables) are the angular velocities ω_e, ω_m and ω_w, respectively the speeds of the internal combustion engine shaft, of the electric motor shaft and of the wheels.

$$\begin{cases} \left({}^{e}J_g + J_e\right)\dot{\omega}_e = T_e - {}^{e}T_g + {}^{e}T_s - T_{aux} - T_{fr} \\ J_m\dot{\omega}_m = T_m - {}^{m}T_r \\ J_w\dot{\omega}_w = {}^{w}T_c - T_{rr} \end{cases} \tag{4}$$

J_e, J_g, J_m are, respectively, the total equivalent inertias of the ICE, EG and EM. J_w is the vehicle inertia at the wheel axis. The inertias of the gears and of the shafts are disregarded. The left superscript e stands for a certain quantity related to the engine shaft through a reduction gear. Analogously for the left superscripts m and w. For example ${}^{e}T_g$ stands for the electric generator torque at the engine shaft by considering the reduction gear effect, also in terms of efficiency.

As a matter of fact, unlike [10], [11], we include the gear mechanical efficiencies η to avoid optimistic fuel economy prediction. Let g_g, g_s, g_r, g_c, respectively, be the gear ratios of the generator shaft, solar shaft, ring shaft and carrier shaft. g_f is the final gear ratio before the differential. In the mechanical coupling unit [2]:

$$\begin{cases} \omega_g = g_g\omega_e \\ \omega_s = g_s\omega_e \end{cases} \tag{5}$$

$$\begin{cases} T_g = \frac{\eta^{\beta_g}}{g_g}\ {}^{e}T_g \\ \\ T_s = \frac{\eta^{\beta_s}}{g_s}\ {}^{e}T_s \end{cases} \tag{6}$$

then (the minus sign in the following equation is due to our reference frames), due to the reduction gear g_r and g_f,

$$\begin{cases} \omega_r = -g_r\omega_m \\ \omega_w = g_f\omega_c \end{cases} \tag{7}$$

$$\begin{cases} T_r = \frac{\eta^{\beta_r}}{g_r}\ {}^{m}T_r \\ {}^{w}T_c = \frac{\eta^{\beta_c}}{g_f}\ T_c. \end{cases} \tag{8}$$

The planetary gear speed constraint (1), together with equations (5) and (7), becomes

$$g_s\omega_e = \frac{(1+\rho)}{g_f}\omega_w + \rho g_r\omega_m. \tag{9}$$

Equations (4) turn into

$$\begin{cases} \left({}^{e}J_g + J_e\right)\dot{\omega}_e = T_e - \frac{g_g}{\eta^{\beta_g}}T_g + \frac{g_s}{\eta^{\beta_s}}T_s - T_{aux} - T_{fr} \\ J_m\dot{\omega}_m = T_m - \frac{g_r}{\eta^{\beta_r}}T_r \\ J_w\dot{\omega}_w = \frac{\eta^{\beta_c}}{g_f}T_c - T_{rr}. \end{cases} \tag{10}$$

The exponents β_g, β_s, β_r, $\beta_c \in \{-1, 0, +1\}$ ensure energy losses for all power flow directions. Note that although (10) contains three equations, one velocity is linked to the other two by equation (9). Explicit dependence by internal torques T_r, T_c and T_s can be also eliminated by using the torque constraints (2) and further simplifications, see [11] for details.

To complete the dynamical model of the propulsion system, we need one more state variable that is the battery State of Charge (SOC). Although the internal resistance model [19] is quite a simple representation of the battery dynamics, it was already employed for simulations also in non trivial powertrain models, [20] among others. Let C_b the equivalent battery capacity and I_b the battery current, then the SOC dynamics is

$$\dot{SOC} = -\frac{I_b}{C_b}. \tag{11}$$

With the internal battery resistance R_b, the battery power P_b is

$$P_b = V_{oc}I_b - R_bI_b^2, \tag{12}$$

where V_{oc} is the open circuit voltage, that is a function of the SOC; instead R_b is constant in our battery model. Here when P_b and I_b are both positive, the battery is discharged [11]. Note that we can write P_b as the power balance between the EG power and the EM power:

$$P_b = P_g - P_m = T_g\omega_g\eta_g^{k_g} - T_m\omega_m\eta_m^{k_m}, \tag{13}$$

where η_g, η_m are, respectively, the generator and the motor efficiency; exponent $k_g = +1$ (-1) if the generator works as a generator (motor), while $k_m = -1$ $(+1)$ if the motor works as a motor (generator). The signs for the motor and the generator terms are different because of the sign convention.

By using equation (11), we get the last differential equation of the dynamic model:

$$\dot{SOC} = -\frac{-V_{oc} + \sqrt{V_{oc}^2 - 4R_bP_b}}{2R_bC_b}. \tag{14}$$

III. CONTROL OF THE HYBRID ELECTRIC POWERTRAIN

In this section, a simple control strategy is derived. The control strategy takes advantage of the degrees of freedom introduced by the electrical subsystem of the series-parallel hybrid architecture. The general feedback control scheme is in Figure 3 and it is inspired by the one in [10]. The inputs of the control system are the desired wheel speed ω_w^{ref} and the desired power P_{aux} for the bucket handling.

Firstly a power repartition is performed between the internal combustion engine and the electrical subsystem, depending on the current battery SOC. Therefore a weight function penalises the use of the ICE when the SOC is relatively high, while it penalises the use of the battery stored energy when the SOC is relatively low.

At each time instant, after fixing the desired ICE power $P_e^{ref} = P_e^{ref}(SOC)$ due to the previous repartition, the control strategy uses the EG to regulate the engine torque and the EM to settle the engine speed. The engine responds to the power demand by working in its best efficiency operating point, $T_e^{ref} = T_e^{ref}\left(P_e^{ref}\right)$, $\omega_e^{ref} = \omega_e^{ref}\left(P_e^{ref}\right)$, compatible with the requested engine power (over the P_e^{ref} hyperbole on the ω_e T_e efficiency map). We want the electric generator torque T_g to regulate the engine torque T_e because it is very close to the engine and its torque directly affects the engine shaft dynamics as well expressed in equations (10). Therefore the decoupling task for the proposed series-parallel hybrid electric architecture is simpler than the classical one. Here a PID control law

$$\begin{aligned} T_g(t) = K_{P,g}\left(T_e^{ref}(t) - T_e(t)\right) + \\ + K_{I,g}\int_0^t \left(T_e^{ref}(\tau) - T_e(\tau)\right)d\tau + \\ + K_{D,g}\,\frac{d}{dt}\left(T_e^{ref}(t) - T_e(t)\right) \end{aligned} \quad (15)$$

for regulating the engine torque is adopted.

The EM has the task to help the classic *throttle* PID controller (T_e) in regulating the ICE speed ω_e for all wheel speeds ω_w. In fact, fixing the reference wheel speed ω_w^{ref} and the desired engine speed ω_e^{ref}, the desired EM speed $\omega_m^{ref} = \omega_m^{ref}\left(\omega_e, \omega_w^{ref}\right)$ follows from the constraint (9) of the planetary gear unit. Also for the electric motor torque, a PID controller is used to track the desired speed of the electric motor itself.

$$\begin{aligned} T_m(t) = K_{P,m}\left(\omega_m^{ref}(t) - \omega_m(t)\right) + \\ + K_{I,m}\int_0^t \left(\omega_m^{ref}(\tau) - \omega_m(\tau)\right)d\tau + \\ + K_{D,m}\,\frac{d}{dt}\left(\omega_m^{ref}(t) - \omega_m(t)\right) \end{aligned} \quad (16)$$

The gains $K_{P,g}$, $K_{P,m}$, $K_{D,g}$, $K_{D,m}$, $K_{I,g}$, $K_{I,m}$ of the electric generator and the electric motor are design parameters. As first step, we tuned these controllers for a simplified system dynamics. Having done so, the next step was to retune the controllers as necessary for the nonlinear dynamics through nonlinear simulations.

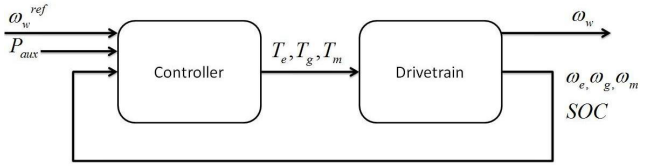

Fig. 3. Control scheme. The control signals are the torques. They regulate the wheel speed and also satisfy the power demand from the bucket handling.

Indeed the electric motor takes care of traction transients and peak power demands. As a result, the operating point of the internal combustion engine is completely decoupled from the vehicle dynamics. Consequently the engine supplies only slowly variable power and its attitude is similar to the one in [21] for small periods of time. In other words, the engine power is not maintained constant, but it can only slowly vary over time, and this is expected to be energy and pollution effective to reduce transients that are normally considered an important cause of excess losses and pollutant emissions [21].

IV. SIMULATIONS

In this section we show numerical simulation results over the industrial vehicle case of study. The loader, pictured in Figure 1, weights 5800 kg and it can carry up to 4000 kg in the bucket. The wheel base is 2.2 m and the wheel radius is 0.53 m. The drivetrain parameters are $g_g = 1.3$, $g_s = 0.33$, $g_r = 0.7$, $g_f = 0.06$ and $\eta = \eta_0 = 0.97$.

The original engine maximum power is 57 kW. By introducing the electric generator and motor, both three-phase alternating current (AC) induction machines of 30 kW and by applying the control strategy, we obtained a possible conservative engine downsizing to 35 kW. Engine power downsizing below 37 kW has an important impact on engine cost, in fact emission standard fulfillment might be achieved with simple, or even no, exhaust gas aftertreatment systems.

Engine efficiency and consumption maps have been provided by the Diesel engine supplier. The electric generator and motor models are first order systems with typical efficiency and maximum power maps (linear maximum power region and constant maximum power region, separated by the base speed). EG, EM and battery parameters, R_b, $C_b = 4\ Ah$ (Ampere hour), have been taken from their data sheets. The rolling resistance torque T_{rr} is an affine function of the vehicle mass (plus the load mass) and of the wheel speed ω_w. The parameters of this law derive from experimental tests on the vehicle.

The loader powertrain is simulated over a standard Y duty cycle, modeled as in [22]. Its qualitative profile is shown in Figure 4. The Y cycle takes his name from the Y-shaped path followed in the horizontal plane by loaders, in their usual employment. In the first half of the duty cycle the vehicle is unloaded and it moves forward to reach the point for the bucket filling. In the filling phase, the loader moves forward at a very

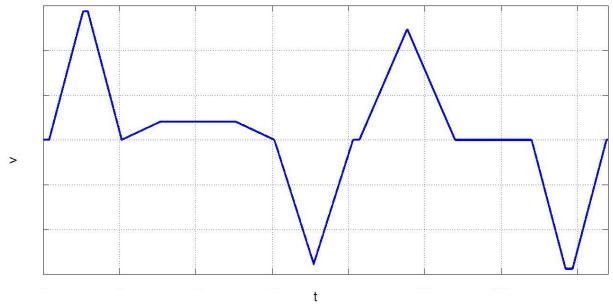

Fig. 4. The duty cycle of the longitudinal vehicle speed has both forward and backwards phases. The bucket filling phase is performed at extremely low speed.

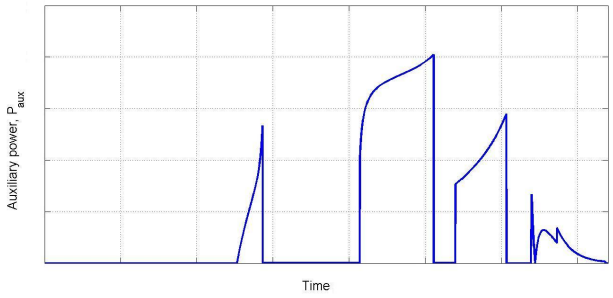

Fig. 5. Auxiliary power demand for the bucket handling.

low speed. When the bucket is loaded, the vehicle can move backwards and then forward to the point where it has to empty the bucket. Finally the unloaded vehicle moves backwards returning back to its initial position. Other examples of Y cycles can be found in [16]. The auxiliary power demand due to the bucket handling is usually unsmooth and it is shown in Figure 5.

Figure 6 shows the ICE operating points in the engine efficiency map. It can be seen that the control strategy works well in regulating the ICE in its optimal curve in terms of efficiency with respect to a fixed requested power. One could think that it would be better if we always control the ICE in its higher efficiency (about 39% at ω_e in the range [1800-2000] rpm and maximum T_e) operating region, but the medium requested power over a duty cycle is quite small, so, obviously, the mentioned region would determine higher fuel consumption, as can could be seen in the fuel consumption engine map.

In Figures 7 and 8 we can see that the EM preserves the ICE from the peak power demands as desired. The propulsion system usually works as a series hybrid electric powertrain and for small intervals of time the engine power directly reaches the wheels through the planetary gear unit (parallel architecture behavior). In Figure 9 the qualitative behavior of the powers of interest over two duty cycles is shown. The battery SOC is mantained inside the 40-60$\%$ values.

We have also modeled and simulated the conventional hydrostatic powertrain for the wheel loader case of study, with

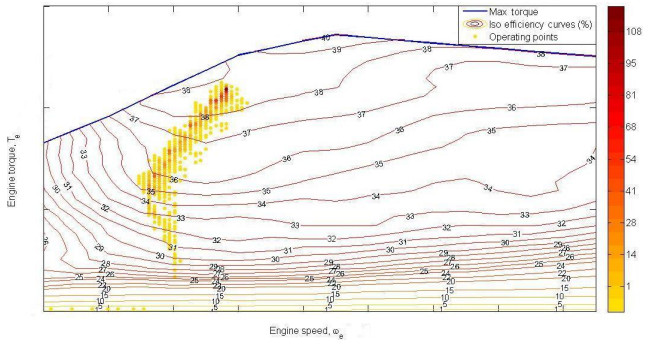

Fig. 6. Operating points of ten duty cycles on the engine efficiency map. Darker is the point higher is the frequency associated to it. In the x axis the engine angular velocity ω_e in round per minute (rpm) and in the y axis the engine torque in Nm.

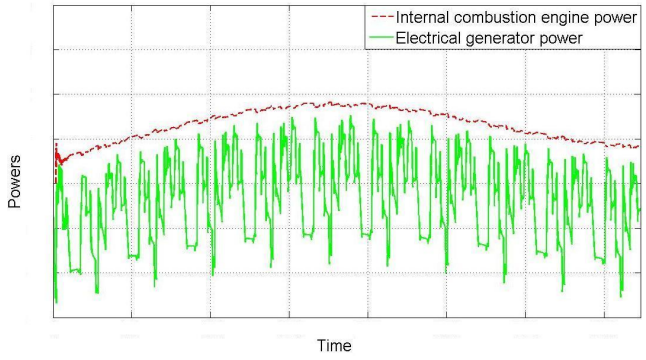

Fig. 7. Thermal engine and electric generator powers over ten duty cycles. The internal combustion engine is not so much affected by transients, due to the unsmooth direct assistance of the electric generator.

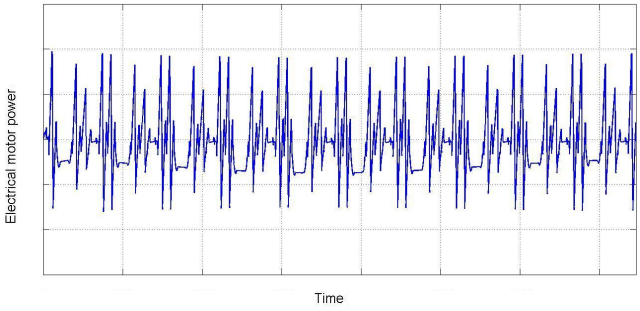

Fig. 8. Electric motor power over ten duty cycles.

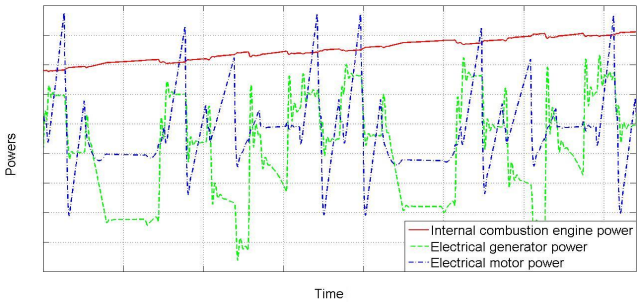

Fig. 9. ICE, EG, EM powers over two duty cycles.

the same vehicle, engine and drivetrain parameters, besides experimental efficiency maps of hydrostatic pump and motor. The description of the hydrostatic powertrain goes behind the aim of this work, therefore it is not presented here, also because of space limitations. The interested reader is referred to recent works in modeling hydrostatic Continuously Variable Transmissions (CVTs) for propulsions systems, such as [15], [16] and the references therein. We tested three different Y duty cycles (short, medium and long range), ten times each. All of them share the qualitative behavior of Figures 4, 5. Simulation comparisons between the proposed series-parallel hybrid electric powertrain and the hydrostatic propulsion point out that the hybrid electric solution reduces the fuel consumption of about 12% (from 10% to 15%, it depends on the specific performed duty cycle) with respect to the conventional hydrostatic one. In our opinion, this favorable result is actually due to the additional degrees of freedom introduced by the electrical subsystem, while for the hydrostatic transmission we can only place the most efficient operative point of the transmission near a speed that is frequently traveled during the vehicle duty cycle (from [15]).

V. Conclusion

Considering ordinary employments of front-end loaders, an input-coupling output-split series-parallel hybrid electric architecture is presented. This solution is novel for off-road vehicles. The control strategy leads the engine in its high efficiency operating regions depending on the power requests and the battery state of charge. The control task is decoupled between engine torque control by the electric generator and the speed control by the electric motor, in an easier way with respect to the classic series-parallel architectures. Except for the application of the input-coupled output-split series-parallel hybrid electric powertrain to off-road trucks, many tools of the present paper have been already studied and developed in the literature. However they have not ever been used all together for the propulsion system of an industrial vehicle. Therefore the goal of this work is to apply the tools commonly used for modeling hybrid electric automotive powertrains to show a promising field of application, i.e. the one of industrial loaders. Simulations show attractiveness of the proposed propulsion system for engine downsizing and peak power preserving, besides fuel economy purposes. From this point of view, simulations results show that the proposed hybrid electric powertrain overcome the performances of the classic hydrostatic propulsion, at least for the class of loaders case of study.

A future line of research will be the study of optimization techniques for the control strategy of the hybrid electric powertrain. In particular, the implementation of the *Pontryagin's maximum principle* and the comparison with sub-optimal control strategies will be considered.

References

[1] Y. Gao and M. Ehsani, *A torque and speed coupling hybrid drivetrain architecture, control, and simulation*, IEEE Trans. on Power Electronics, vol. 21, n. 3, 2006.

[2] M. Ehsani, Y. Gao, S. Gay, and A. Emadi, *Modern electric, hybrid electric and fuel cell vehicles: fundamentals, theory, and design*, CRC Press LLC, 2004.

[3] A. Brahma, Y. Guezennec and G. Rizzoni, *Optimal energy management in series hybrid electric vehicles*, Proc. of the American Control Conference, Chicago, Illinois, 2000.

[4] S. Barsali, C. Miulli and A. Possenti, *A control strategy to minimize fuel consumption of series hybrid electric vehicles*, IEEE Trans. on Energy Conversion, vol. 19, n. 1, 2004.

[5] P. Pisu and G. Rizzoni, *A supervisory control strategy for series hybrid electric vehicles with two energy storage systems*, IEEE Vehicle Power and Propulsion Conference, Chicago, Illinois, 2005.

[6] L. Serrao and G. Rizzoni, *Optimal control of power split for a hybrid refuse vehicle*, Proc. of the American Control Conference, Seattle, Washington, 2008.

[7] A. Brahma, Y. Guezennec and G. Rizzoni, *Dynamic optimization of mechanical/electrical power flow in parallel hybrid electric vehicles*, Proc. of the Int. Symp. on Advanced Vehicle Control, Ann Arbor, Michigan, 2000.

[8] C. C. Lin, J. M. Kang, J. W. Grizzle and H. Peng, *Energy management strategy for a parallel hybrid electric truck*, Proc. of the American Control Conference, Arlington, Virginia, 2001.

[9] S. Delprat, J. Lauber, T. M. Guerra and J. Rimaux, *Control of a parallel hybrid powertrain: optimal control*, IEEE Trans. on Vehicular Technology, vol. 53, n. 3, 2004.

[10] J. Liu, H. Peng and Z. Filipi, *Modeling and analysis of the Toyota Hybrid System*, Proc. of the IEEE/ASME Int. Conf. on Advanced Intelligent Mechatronics, Monterey, California, 2005.

[11] J. Liu and H. Peng, *Control optimization for a power-split hybrid vehicle*, Proc. of the American Control Conference, Minneapolis, Minnesota, 2006.

[12] A. Sciarretta and L. Guzzella, *Control of hybrid electric vehicles*, IEEE Control Systems Magazine, pp. 60-70, April 2007.

[13] C. Musardo, G. Rizzoni and B. Staccia, *A-ECMS: an adaptive algorithm for hybrid electric vehicle energy management*, Proc. of the IEEE Conf. on Decision and Control and the European Control Conference, Seville, Spain, 2005.

[14] L. Serrao, S. Onori and G. Rizzoni, *ECMS as a realization of Pontryagin's minimum principle for HEV control*, Proc. of the American Control Conference, St. Louis, Missouri, 2009.

[15] B. Carl, M. Ivantysynova and K. Williams, *Comparison of operational characteristics in power split continuously variable transmissions*, SAE paper 2006-01-3468, 2006.

[16] R. Kumar, M. Ivantysynova and K. Williams, *Study of energetic characteristics in power split drives for on highway trucks and wheel loaders*, SAE paper 2007-01-4193, 2007.

[17] John M. Miller, *Hybrid electric vehicle propulsion system architectures of the e-CVT type*, IEEE Trans. on Power Electronics, vol. 21, n. 3, pp. 756767, 2006.

[18] L. Guzzella and A. Sciarretta, *Vehicle propulsion systems: introduction to modeling and optimization*, Springer, 2007.

[19] O. Tremblay, L. A. Dessaint and A. I. Dekkiche, *A generic battery model for the dynamic for dynamic simulations of hybrid electric vehicles*, IEEE Vehicle Power and Propulsion Conference, Arlington, Texas, 2007.

[20] Z. Han, Z. Yuan, T. Guangyu, C. Quanshi and C. Yaobin, *Optimal energy management strategy for hybrid electric vehicles*, SAE paper 2004-01-0576, 2004.

[21] M. Ceraolo, A. di Donato and G. Franceschi, *Energy optimization of hybrid-electric vehicles. The Pisa experience*, IEEE Vehicular Power and Propulsion Conference, Windsor, United Kingdom, 2006.

[22] R. Filla, *An event-driven operator model for dynamic simulation of construction machinery*, Scandinavian International Conference on Fluid Power, Linköping, Sweden, 2005.